# The Internal Rotation of Hydrogen Thioperoxide: Energy, Chemical Potential, and Hardness Profiles

**Gloria I. Cárdenas-Jirón**

*Departamento de Química de los Materiales, Facultad de Química y Biología, Universidad de Santiago de Chile, Casilla 40, Correo 33, Santiago, Chile*

**Jorge Ricardo Letelier**

*Departamento de Química, F.C.F.M., Universidad de Chile, Casilla 2777, Santiago, Chile*

**Alejandro Toro-Labbé***

*Departamento de Química Física, Facultad de Química, Pontificia Universidad Católica de Chile, Casilla 306, Correo 22, Santiago, Chile*

*Received: April 14, 1998; In Final Form: July 10, 1998*

We present a theoretical study of the internal rotation of HSOH. Calculations at the ab initio HF//6-311G** level show that HSOH is a gauche molecule presenting a *double-barrier* torsional potential. The different mechanisms associated with isomerization passing by a trans or a cis barrier have been characterized with the use of the profiles of potential energy ($V$), electronic chemical potential ($\mu$), and molecular hardness ($\eta$). Important results have been obtained: (a) the principle of maximum hardness is verified; (b) the profiles of $\mu$ and $\eta$ in connection with that of local electronic populations allows one a qualitative characterization of the nature of the two potential barriers hindering the internal rotation.

## 1. Introduction

In this paper we are concerned with the study of the internal rotation process in hydrogen thioperoxide from the perspective of the simultaneous evolution of the potential energy ($V$), the electronic chemical potential ($\mu$), and the molecular hardness ($\eta$). Along the torsional angle HSOH presents the interesting feature of having a single well with two energy barriers. This allows one to study, in a single molecule, the different isomerization paths in terms of specific mechanisms and local interactions. This give insights about the nature of the potential barriers.

Density functional theory (DFT) has provided the theoretical basis for concepts that are implicated in the reactivity of chemical species. The electronic chemical potential characterizes the escaping tendency of electrons from the equilibrium system, and the molecular hardness can be seen as a resistance to charge transfer.[1−6] Both are global properties of the system, and the characterization of their profiles along a reaction coordinate has been shown to be useful to study new aspects of the progress of chemical reactions.[7−10]

One major focus of attention in DFT is the principle of maximum hardness (PMH) that asserts that molecular systems at equilibrium tend to states of high hardness;[4,11−13] transition states should therefore present a minimum value of hardness. We have shown recently that the search of consistency between the PMH and the Hammond postulate[14] may lead to a better characterization of transition states.[9] Although Parr and Chattaraj[15] showed that the PMH holds under the constraints that the external potential and the electronic chemical potential must remain constant upon distortion of the molecular structure, it seems to be valid even under less severe conditions than the ones stated above. Relaxation of the constraints seems to be permissible, and in particular it has been found that the PMH still holds even though the electronic chemical potential strongly varies along a reaction coordinate.[8−10,12,16−18] For more details about this point, we refer the reader to the review on the PMH by P. K. Chattaraj[11] and to the excellent account on the molecular hardness concept by R. G. Pearson.[12]

The aim of this paper is 2-fold; on one side it is methodological because there is a theoretical model that we use to relate $\mu$, $\eta$, and $V$[8−10] and also because we test the quality of different theoretical procedures to compute the electronic properties. On the other side, we want to contribute to the knowledge of HSOH, a molecule that is thought to participate as an intermediate in atmospheric reactions leading to depletion of ozone and in various processes associated with the atmospheric oxidation of sulfides, one of the chemical processes that leads to acid rain.[19,20]

We have mentioned that in its electronic ground state HSOH is a gauche molecule with two barriers for internal rotation that are located at the planar trans and cis conformations.[21] There is experimental evidence for the existence of hydrogen thioperoxide in an argon matrix[22] and in the gas phase.[23] From a theoretical viewpoint HSOH has been little studied. Few papers have been published, most of them aimed at studying the molecular structure and gas-phase acidities and to characterize the thermochemistry of its radicals.[21,24−27] HSOH presents two planar conformers, cis and trans, which are higher in energy with respect to the gauche stable conformation.

The paper is organized as follows. In section 2 we present the model relating $\mu$, $\eta$, and $V$ along the reaction coordinate. In section 3 we present and discuss our results, and section 4 contains our concluding remarks.

* Author for correspondence. E-mail: atola@puc.cl.

S1089-5639(98)01841-6 CCC: $15.00 
Published on Web 09/12/1998

## 2. Theoretical Background

The reaction coordinate is the torsional angle α defined with respect to the SO bond and measured from the trans (α = 0) to the cis (α = π) conformations. The potential function hindering the internal rotation of HSOH in the α representation is given by[8−10]

$$V(\alpha) = \frac{1}{4}K_V(1 - \cos^2\alpha) + \frac{1}{2}\Delta V^\circ(1 - \cos\alpha) \qquad (1)$$

where $K_V$ is a parameter associated with the reference conformations and $\Delta V^\circ = (V(\pi) - V(0))$ is the energy difference between them.

It has been shown that it is useful to define a reduced reaction coordinate measuring the reaction progress when going from reactants to products. The reduced coordinate, $\omega$, which has been called *conformational function*, is related to the torsional angle α through $\omega = (1 - \cos\alpha)/2$; it varies from zero (trans) to one (cis). The functional defining the potential energy in the $\omega$ representation is given by[8−10]

$$V[\omega] = K_V f[\omega] + \omega\Delta V^\circ \qquad (2)$$

where $f[\omega] = \omega(1 - \omega)$ is obtained by replacing the definition of $\omega$ in eq 1. The definition of $\mu$ and $\eta$ were given by Parr and Pearson,[2] and a three-points finite difference approximation leads to the following working definitions of these quantities

$$\mu = -\frac{1}{2}(\mathrm{IP} + \mathrm{EA}); \quad \eta = \frac{1}{2}(\mathrm{IP} - \mathrm{EA}) \qquad (3)$$

IP and EA are the first vertical ionization potential and electron affinity of the neutral molecule, respectively. The Koopmans' theorem (IP ≈ $-E_\mathrm{H}$ and EA ≈ $-E_\mathrm{L}$) allows one to write $\mu$ and $\eta$ in terms of the energy of frontier HOMO ($E_\mathrm{H}$) and LUMO ($E_\mathrm{L}$) molecular orbitals

$$\mu = \frac{1}{2}(E_\mathrm{L} + E_\mathrm{H}); \quad \eta = \frac{1}{2}(E_\mathrm{L} - E_\mathrm{H}) \qquad (4)$$

Determination of $\mu$ and $\eta$ from quantum chemistry involves a different kind of calculations; a ΔSCF procedure should be used when applying eq 3, and the Koopmans' theorem is implicit in eq 4. Reliability and estability of numerical results obtained through different methodologies will be analyzed in the next section. Now, since $\mu$ and $\eta$ are global properties of the system, their evolution along the reaction coordinate (α or $\omega$) is correctly represented through the same analytic form already used for the torsional potential ($V(\alpha)$ or $V[\omega]$). Therefore, for the chemical potential we can write

$$\mu[\omega] = \mu[0] + K_\mu f[\omega] + \omega\Delta\mu^\circ \qquad (5)$$

and for the molecular hardness

$$\eta[\omega] = \eta[0] + K_\eta f[\omega] + \omega\Delta\eta^\circ \qquad (6)$$

The parameters ($\Delta\mu^\circ$, $K_\mu$) and ($\Delta\eta^\circ$, $K_\eta$) have the same meaning that ($\Delta V^\circ$, $K_V$) have for $V[\omega]$. We have shown that the numerical values of these parameters can be obtained following a prescription we give in previous works.[8−10] If we use $\Delta\mu[\omega] = (\mu[\omega] - \mu[0])$ and $\Delta\eta[\omega] = (\eta[\omega] - \eta[0])$, combination of eqs 2, 5, and 6 leads to

$$V_\eta[\omega] = \omega\Delta V^\circ + Q_\eta(\Delta\mu[\omega] - \omega\Delta\mu^\circ) \qquad (7)$$

$$V_\mu[\omega] = \omega\Delta V^\circ + Q_\mu(\Delta\eta[\omega] - \omega\Delta\eta^\circ) \qquad (8)$$

and

$$\Delta\mu[\omega] = \omega\Delta\mu^\circ + Q(\Delta\eta[\omega] - \omega\Delta\eta^\circ) \qquad (9)$$

where $Q_\eta = K_V/K_\mu$, $Q_\mu = K_V/K_\eta$, and $Q = Q_\mu/Q_\eta$.[10] From the above expressions, it is possible to obtain a global equation accounting for the simultaneous evolution of the three properties along a reaction coordinate, and combination of eqs 7 and 8 yields

$$V[\omega] \equiv \frac{1}{2}(V_\eta[\omega] + V_\mu[\omega]) = \omega\Delta V^\circ + \frac{1}{2}Q_\eta(\Delta\mu[\omega] - \omega\Delta\mu^\circ) + \frac{1}{2}Q_\mu(\Delta\eta[\omega] - \omega\Delta\eta^\circ) \qquad (10)$$

This is an interesting equation because it combines energetic ($V$) with mechanistics aspects (included in $\mu$ and $\eta$) of the dynamical process. The position of the stable isomer can be determined by differentiating eq 1 or 2 such that $(dV/d\omega)_{\omega=\beta} = 0$. $\beta$ is the position of the gauche conformation and, defined in terms of the potential energy parameters, is given by

$$\beta = \frac{1}{2} + \frac{\Delta V^\circ}{2K_V} \qquad (11)$$

Putting $\beta$ in eq 1 or 2 yields the following expression for the energy of the gauche isomer, and the negative of it corresponds to the trans potential barrier

$$\Delta V^\ddagger \equiv -V[\beta] = -\left(\frac{1}{4}K_V + \frac{1}{2}\Delta V^\circ + \frac{(\Delta V^\circ)^2}{4K_V}\right) \qquad (12)$$

By evaluating eq 10 in $\omega = \beta$ we obtain an alternative expression for the trans activation energy, now in terms of the activation chemical potential ($\Delta\mu^\ddagger \equiv \Delta\mu[\beta]$) and the activation hardness ($\Delta\eta^\ddagger \equiv \Delta\eta[\beta]$)

$$\Delta V^\ddagger = -\left(\beta\Delta V^\circ + \frac{1}{2}Q_\eta(\Delta\mu^\ddagger - \beta\Delta\mu^\circ) + \frac{1}{2}Q_\mu(\Delta\eta^\ddagger - \beta\Delta\eta^\circ)\right) \qquad (13)$$

This equation connects the three activation properties through the parameters $Q_\eta$ and $Q_\mu$, it might provide new interpretations of the nature of activation energies, and certainly it may help to give new insights about reaction mechanisms. It is important to mention that for different types of reactions it has been found that $\mu$ and $\eta$ pass through an extrema at $\beta$ or very near to it;[8−10] this ensures that eq 13 produces reliable values of potential barriers from the knowledge of activation electronic properties.

On the other hand, it should be pointed out that eq 12 is structurally homogeneous to the Marcus equation originally proposed to characterize electron-transfer processes[28] and later on used for interpretation of different kinds of chemical reactions.[29] A term-to-term comparison of these two equations shows that $^1/_4$ $K_V$ is associated with the Marcus' *intrinsic activation energy* ($\Delta V_0^\ddagger$). At this point we can explore further implications of this term, and according to eq 13, the intrinsic activation energy can be written as

$$\frac{1}{4}K_V \equiv \Delta V_0^\ddagger = \frac{(\Delta V^\circ)^2}{4K_V} + \frac{1}{2}Q_\eta(\Delta\mu^\ddagger - \beta\Delta\mu^\circ) + \frac{1}{2}Q_\mu(\Delta\eta^\ddagger - \beta\Delta\eta^\circ) \qquad (14)$$

Since the first term that includes the exothermicity of the reaction is normally smaller than the other two terms, it is possible to give a physical interpretation of the Marcus' intrinsic activation energy: it arise from the electronic properties $\mu$ and $\eta$, and therefore it should be fully characterized from the analysis of the electronic density.

### 3. Results and Discussion

The profiles of $V$, $\mu$, and $\eta$ were obtained through SCF ab initio calculations at the RHF level with the standard 6- -311G** basis set using the Gaussian 94 package.[30] The force gradient method with analytical gradient was used for full optimization of the structural parameters every 10° along the torsional angle $\alpha$. In addition to this, since $\mu$ and $\eta$ were also estimated following a $\Delta$SCF procedure, extra calculations were performed using the UHF and ROHF theories.

**3.1. Molecular Structure.** The optimized geometrical parameters at the HF/6-311G** level for the gauche stable conformation are $R$(SO) = 1.652 Å, $R$(SH) = 1.333 Å, $R$(OH) = 0.942 Å, $\angle$(HSO) = 98.7°, $\angle$(HOS) = 109.1°, and dihedral angle $\angle$(HSOH) = 91.2°. Note that the optimized position of the gauche stable conformation along the torsional angle is given by $\alpha = \pi - 91.2°$. Although infrared absorption assigned to HSOH has been recorded[20] and the technique of neutralization−reionization mass spectrometry (NRMS) has been used to identify the molecule in the gas phase,[23] no experimental data are available concerning the equilibrium geometry. However, it is important to point out that our theoretical estimation for the structural parameters of HSOH are in quite good agreement with the experimental geometrical parameters extracted from the parent HOOH and HSSH molecules.[20]

**3.2. Determination of $\mu$ and $\eta$.** The aim of this section is to study the effect of the methodology employed on the numerical values of $\mu$ and $\eta$. For this purpose we compare results determined by means of two different methodologies. The first one is the $\Delta$SCF procedure in which the IP and EA values of eqs 3 are evaluated by carrying out separate SCF calculations for ions at the relaxed geometry of the neutral molecule. The corresponding open shell systems were calculated using both the UHF and ROHF theories. The second methodology we use to determine $\mu$ and $\eta$ consists of application of eqs 4 with $E_H$ and $E_L$ obtained from the RHF calculation on the neutral molecule. It should be noted that both methods to estimate $\mu$ and $\eta$ include errors from electronic correlation and relaxation effects or arising from inadequacy of the Koopmans' theorem.

Figure 1 shows the change of $\mu$ and $\eta$ along $\alpha$. As already mentioned, numerical values were obtained through eqs 3 (curves labeled $\Delta$SCF(UHF) and $\Delta$SCF(ROHF)) and 4 (curve labeled RHF). For comparison purposes, we display the calculated RHF curves along with the corresponding fitted ones. It is found that the analytic forms we use in this paper represent correctly the main features of the evolution of $\mu$ and $\eta$ along the reaction coordinate. Similar favorable comparisons are expected for the ROHF and UHF calculations.

Concerning the comparison among different methodologies, we first note that they show the same qualitative trend. Numerically the RHF values differs considerably with respect to the ones determined from the $\Delta$SCF procedure. The fact that the $\mu$(RHF)'s are smaller than the ones determined from the $\Delta$SCF procedure and that the $\eta$(RHF)'s are larger than the $\Delta$SCF ones, is indicates that the use of $E_L$'s to estimate EA's is not as appropiate as it is the use of $E_H$'s to estimate IP's. This observation is confirmed in Figure 2 where we display

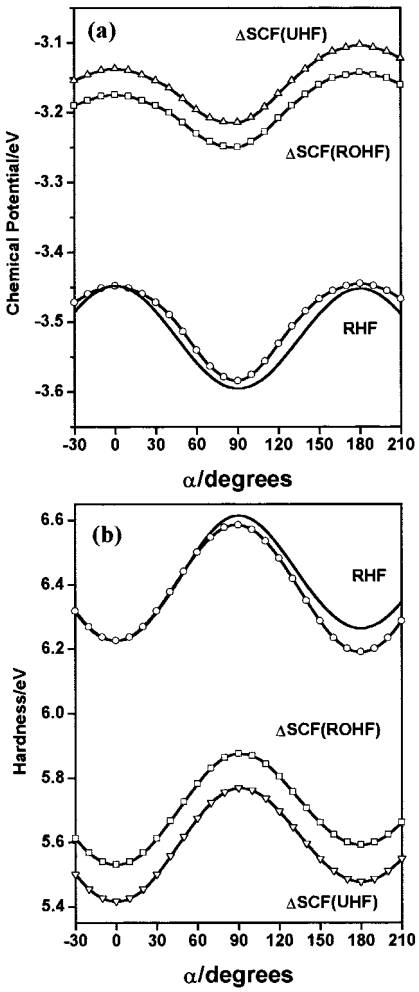


**Figure 1.** Evolution along the torsional angle $\alpha$ of the chemical potential (a) and hardness (b) calculated following different procedures. The RHF fitted curves (no symbols) are also included. All values are given in eV.

the IP's and EA's against the frontier HOMO and LUMO orbitals. We note that ROHF and UHF results follow practically the same behavior. Very good correlations between the IP's and HOMO's are obtained whereas correlations between the EA's and the LUMO's are not so good. Our results support the fact that RHF calculations produce quite good estimations of ionization potentials but they are less appropiate in estimating electron affinities.

A corollary of Figure 1 is that UHF and RHF results are defining upper and lower limits for $\mu$ and $\eta$. In Figure 3 we show that these limiting values are quite well correlated along the reaction coordinate. These correlations for $\mu$ and $\eta$ shows that different methodologies lead to similar qualitative results; these are in turn quantitatively related through a simple two-parameter linear regression. Hardness shows a significantly better correlation than the chemical potential; however, the $\mu$ values estimated through the UHF and RHF methods are numerically closer to each other than are the hardness values, as shown in the insets. In summary, the three methodologies we have used here lead to the same qualitative behavior of $\mu$ and $\eta$ along the reaction coordinate, the numerical values of these properties were found to be related to each other through linear relations. Similar conclusions have been reached by other authors regarding the molecular hardness.[31−33] Chattaraj et al.[32,33] observed that although the numerical values may differ, the overall trends remains unaltered when $\eta$ is calculated using

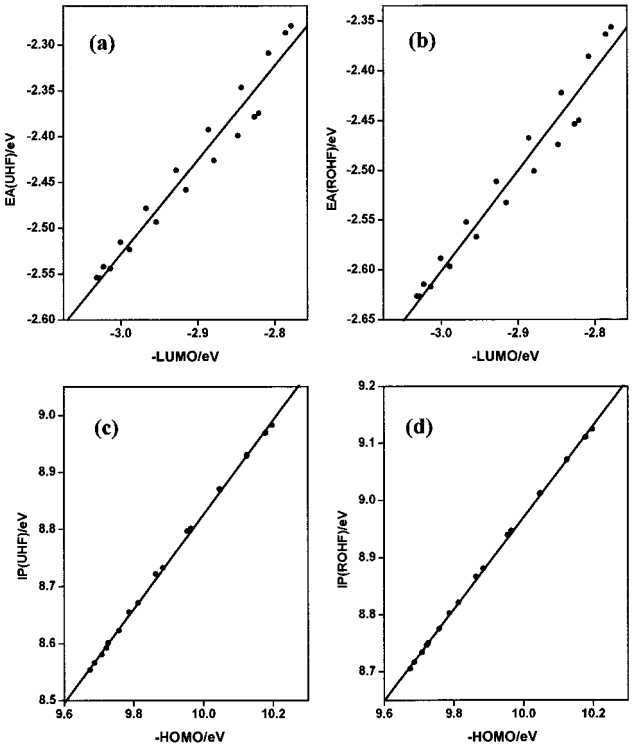


**Figure 2.** Linear correlations between UHF electron affinities and ionization potentials with the RHF LUMO and HOMO energies. The points represent the calculated values along the reaction coordinate. All values are in eV.

either eqs 3 or 4. In light of the above results, only the RHF results for $\mu$ and $\eta$ will be retained for discussion in the remainder of the paper.

**3.3. Electronic Correlation Effects.** The results discussed in the previous paragraphs consider the relaxation effects only; the electronic correlation is not included. A rough estimation of correlation effects can be obtained from post Hartree−Fock calculations. We have performed MP2 calculations with full geometry optimization at each point of the reaction coordinate. These calculations led us to obtain the torsional potential, chemical potential, and molecular hardness at the MP2 level. The latter properties were calculated through eq 4, and the results are displayed in Figure 4, where for comparison purposes we have also included the corresponding RHF values.

Although not displayed here, the overall effect of electronic correlation is to lower the energy by an average amount of about 0.34 au. The energies of Figure 4a are relative to the trans value, and so we observe that only the cis barrier height is affected by correlation; it is increased by about 0.60 kcal/mol. In Figure 4b we note that correlation effects appear to be quite important in the evaluation of chemical potential. Although the general feature is the same, MP2 calculations lead to lower $\mu$ values than the ones estimated through the RHF calculations, and a difference of about 0.18 eV is reached in the trans region. In contrast to this, Figure 4c shows that the effect of electronic correlation on the molecular hardness is quite negligable; it can be distinguished only in the trans region. It is interesting to note that correlation has a global effect on $\mu$ but a local effect on $\eta$. The correlation effect tends to lower the energy of both frontier HOMO and LUMO molecular orbitals. However, since the lowering does not occur homogeneously by about the same amount of energy along the reaction coordinate, it appears that the global correlation effect is large in $\mu$ but less in $\eta$.

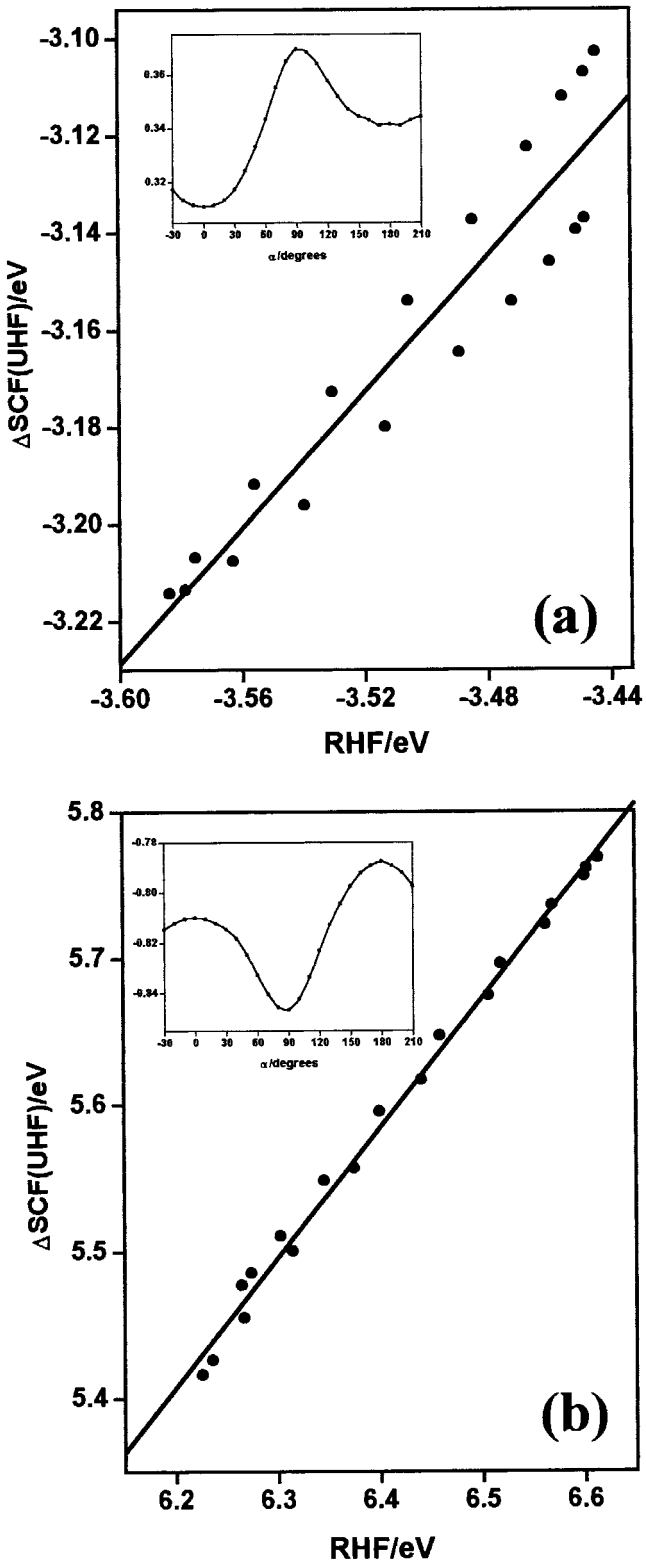


**Figure 3.** Comparison between ΔSCF(UHF) and RHF procedures to calculate $\mu$ (a) and $\eta$ (b). The insets show the deviations with respect to each other.

**3.4. The Principle of Maximum Hardness.** In Figure 5 we provide an illustration of the validity of the PMH. It shows both the torsional potential and the molecular hardness along the reaction coordinate α. In agreement with the PMH, it can be seen that the energy minimum is associated with a hardness maximum whereas energy maxima are connected with hardness minima. It is clear that, as pointed out by Chattaraj,[11] the

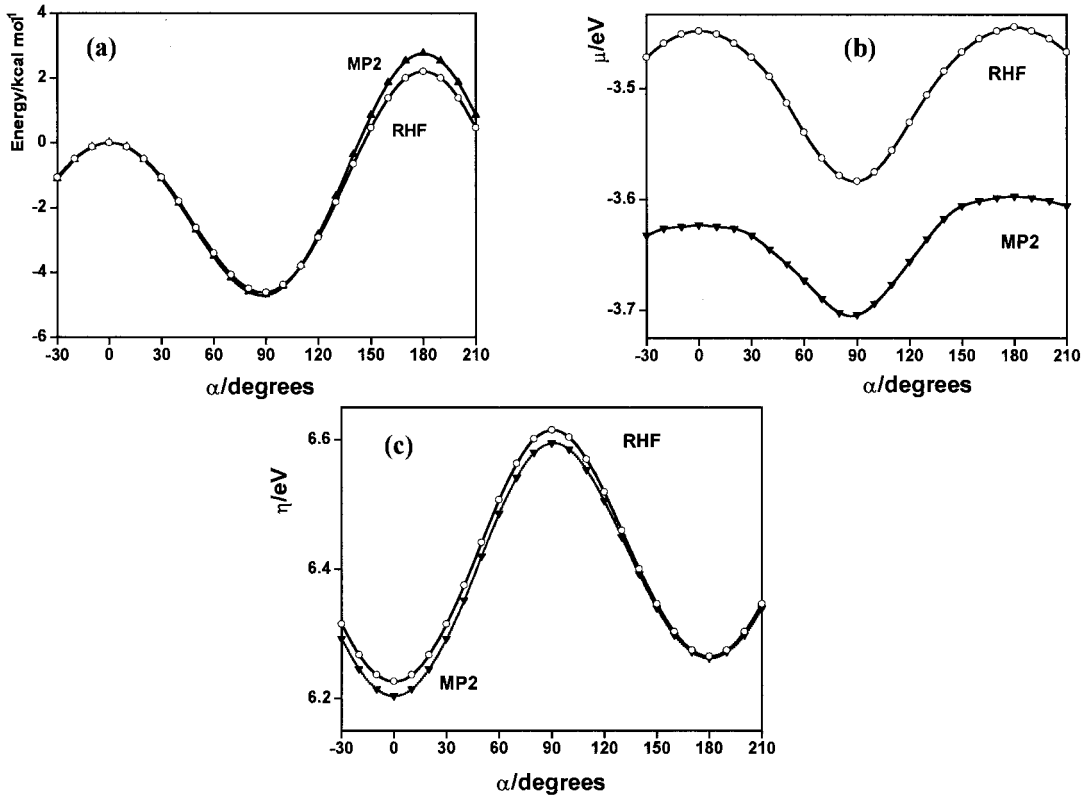


**Figure 4.** Effect of electronic correlation on the torsional potential (a), chemical potential (b), and molecular hardness (c).

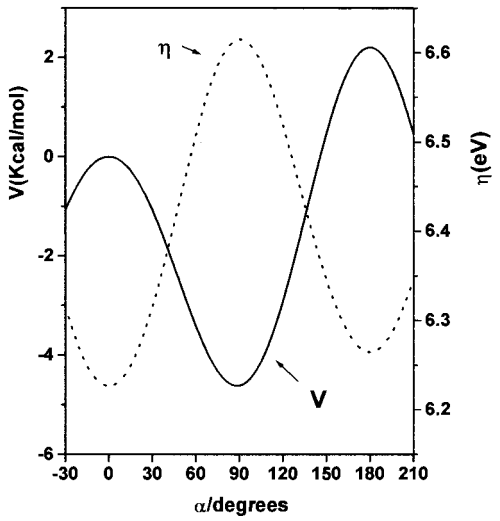


**Figure 5.** Simultaneous evolution of the torsional potential and hardness along α.

maximum hardness condition complements the minimum energy criterion for molecular stability.

**3.5. The Relation between $\mu$, $\eta$, and $V$.** Figure 6 shows a 3D plot of the simultaneous evolution of the isomerization process in the $\{\mu, \eta, V\}$ space; included in the plot are the three projections onto the respective planes. The 3D curve can be rationalized through eq 10, whereas the resulting projections obey eqs 7−9. These equations have been used to fit the RHF numerical values, and the resulting parameters are quoted in Table 1, together with the reference values determined directly from the calculations. Figure 6 shows that the trajectories defined by the torsional motion to go from the stable conformation to either of the planar conformations (transition states) are different in nature. Any departure from the stable conformation will produce a change in the molecular properties; in particular, the escaping tendency of electrons will be favored ($\mu$ increases), and the resistance to charge tranfer will decreases ($\eta$ decreases). With the help of Figure 6 it is possible to make a qualitative difference among the reaction mechanisms defining the cis and trans paths; this can be done through the analysis of the slopes associated with them. We note that $|(\partial V/\partial\mu)_{cis}| > |(\partial V/\partial\mu)_{trans}|$ and $|(\partial V/\partial\eta)_{cis}| > |(\partial V/\partial\eta)_{trans}|$; this indicates that the rearrangement and polarization of the electronic density is faster in the cis path than in the trans path. Therefore, the cis path should be associated mainly with through space interactions whereas the trans path should be characterized by through bond interactions. These qualitative observation will be confirmed in section 3.7 with the analysis of the bond electronic populations in connection with the isomerization mechanisms.

**3.6. Activation Properties.** In Table 2 we collect the activation barriers and the properties defining the gauche conformation. It can be seen that agreement between predicted and optimized values is quite good. The position of the gauche stable conformation is predicted by eq 11 to be at $\beta = 0.46$ in agreement with the optimized value at the RHF level that was $\beta = 0.48$. The trans barrier height predicted through eq 12 is found to be $\Delta V^{\ddagger} = 4.60$ kcal/mol, in very good agreement with the optimized value of 4.62 kcal/mol. Note that the experimental trans barrier for the parent HOOH and HSSH molecules are 1.10 kcal/mol[34] and 5.82 kcal/mol,[35] respectively. The corresponding calculated values at the RHF/6-311G** are 0.87 kcal/mol (HOOH) and 5.65 kcal/mol (HSSH). The trans barrier height for HSOH is expected to be somewhere between the values for these reference molecules; a rough estimation might be the average of the experimental values, 3.46 kcal/mol, which is quite close to our predicted and optimized values considering that the zero-point correction was not included in our estimations.

The chemical potential at the gauche stable conformation is $\Delta\mu(\beta)$ and is obtained from eq 7; the result is −3.58 eV, which

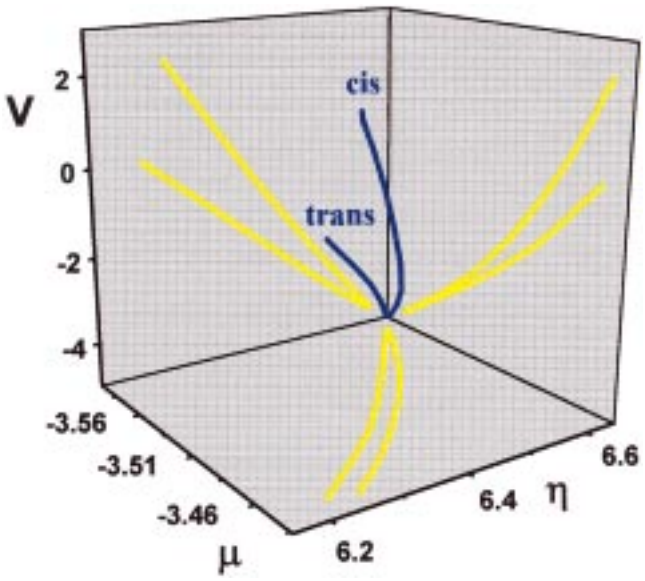


**Figure 6.** 3D representation of the isomerization reaction in the $\{\mu, \eta, V\}$ space. The yellow curves are the projections onto the $\{\mu, V\}$, $\{\mu, \eta\}$, and $\{\eta, V\}$ planes.

**TABLE 1: Fitting Parameters Defining $V$, $\mu$, and $\eta$ Following Eqs 7−10[a]**

| parameter | fitted | calculated |
|---|---|---|
| $K_V$ | −22.29 | −22.13 |
| $\Delta V°$ | 2.04 | 2.21 |
| $K_\mu$ | −0.580 | −0.430 |
| $\Delta\mu°$ | 0.0092 | 0.0037 |
| $\mu[0]$ | −3.4482 | −3.4482 |
| $K_\eta$ | 1.4660 | 1.3039 |
| $\Delta\eta°$ | 0.0360 | 0.0390 |
| $\eta[0]$ | 6.2263 | 6.2263 |
| $Q_\eta$ | 1.6677 | 2.2396 |
| $Q_\mu$ | −0.6598 | −0.7364 |
| $Q$ | −0.3956 | −0.3288 |

[a] The parameters associated with the potential energy are given in kcal/mol; those associated to chemical potential and hardness are given in eV.

**TABLE 2: Activation Barriers and Properties of the Gauche Stable Conformation of HSOH[a]**

| parameter | predicted | optimized |
|---|---|---|
| $\Delta V^{\ddagger}_{trans}$ | 4.60 | 4.62 |
| $\Delta V^{\ddagger}_{cis}$ | 6.64 | 6.83 |
| $\beta$ | 0.46 | 0.48 |
| $V(\beta)$ | −4.60 | −4.62 |
| $\mu(\beta)$ | −3.58 | −3.58 |
| $\eta(\beta)$ | 6.61 | 6.62 |

[a] Potential energies ($V$) are in kcal/mol; $\mu$ and $\eta$ are in eV.

matches exactly the RHF optimized value. Similarly, $\Delta\eta(\beta)$ was determined from eq 8, leading to 6.61 eV, compared with the optimized value of 6.62 eV. The overall good quality of the numerical data produced by eqs 7−10 (see Table 2) indicates the reliability of our model in rationalizing the simultaneous evolution of the energy, chemical potential, and hardness.

**3.7. Bond Densities and Isomerization Mechanisms.** To get more insight into the torsional mechanism, a quantitative characterization of the charge density is necessary. We analyze in this section the evolution along $\omega$ of the Mulliken electronic population localized on the bond regions. The total bond electronic population of the molecule is given by:

$$\rho_{bond} = \rho_{SH} + \rho_{SO} + \rho_{OH} \tag{15}$$

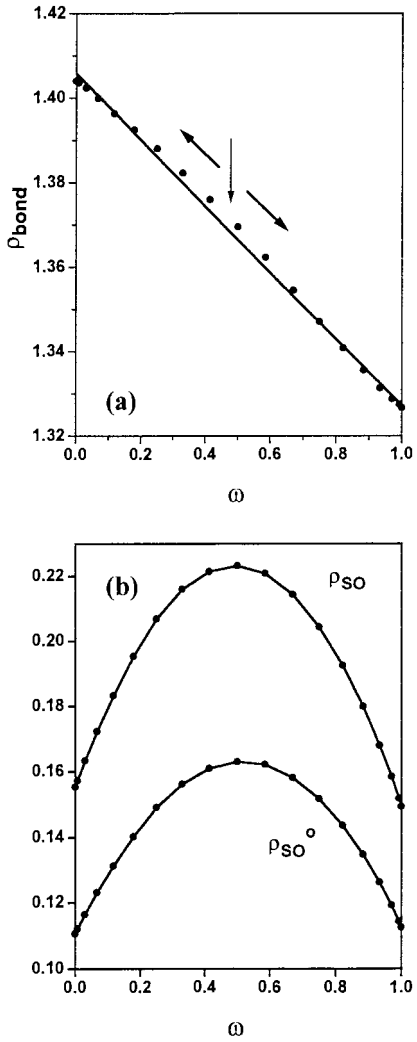


**Figure 7.** Evolution along the reaction coordinate of $\rho_{bond}$ (a) and $\rho_{SO}$ (b). The vertical arrow indicate the stable conformation. The arrow pointing to the left indicates the trans path, whereas the arrow pointing to the right indicates the cis path to isomerization.

where $\rho_x$ is the Mulliken electronic density of the bond $x$ in the molecule. The relative electronic population of the SO central bond is in turn defined as

$$\rho^{\circ}_{SO} = \rho_{SO}/\rho_{bond} \tag{16}$$

In Figure 7 we display the evolution of $\rho_{bond}$, $\rho_{SO}$, and $\rho^{\circ}_{SO}$ along $\omega$. We note in Figure 7a that $\rho_{bond}$ decreases monotonically when going from trans($\omega = 0.0$) to cis($\omega = 180.0$) whereas both $\rho_{SO}$ and $\rho^{\circ}_{SO}$ show a parabolic behavior with a maximum value at the gauche stable isomer. As pointed out in the analysis of Figure 6 and indicated by the arrows in Figure 7a, when standing at the gauche conformation two reaction paths are possible; the one passing by the trans barrier is accompanied by an increasing bond density. The second path goes by the cis barrier and implies a decreasing bond density. Since there is no change in the total number of electrons during the internal rotation, any change in the electronic population of the bond region must be accompanied by an opposite change in the atomic charges. This simple picture of balanced electronic charges centered on the bond regions or on the atomic center may help understand the nature of the two potential barriers involved in the rotational isomerization process.

Figure 7a in connection with Figure 5, which shows that the trans barrier is smaller than the cis one, indicates that a high

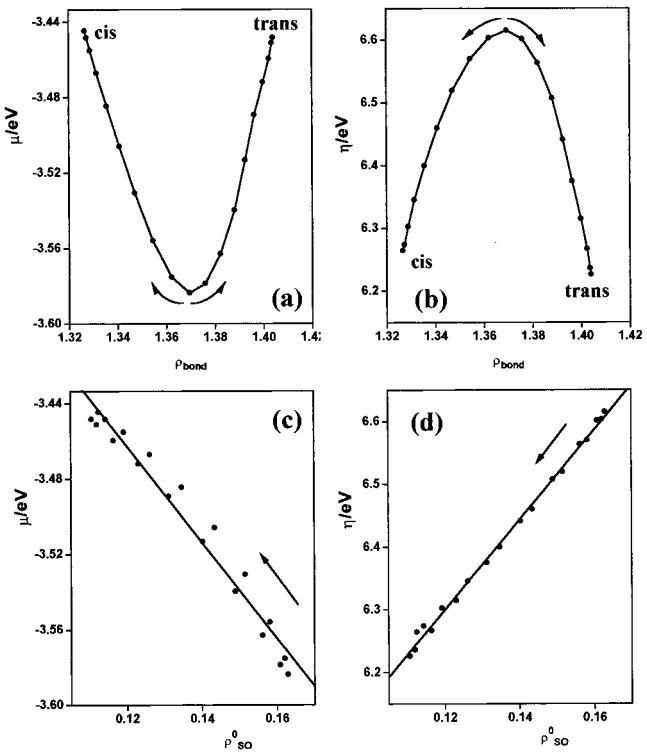


**Figure 8.** Dependence of $\mu$ and $\eta$ with respect to $\rho_{bond}$ and $\rho^{\circ}_{SO}$.

barrier is associated with a decreasing bond density. This must increase the atomic charges, and therefore the cis barrier should be mainly due to electrostatic atom−atom *through space* interactions. In contrast to this picture, the same analysis suggests that the trans barrier is characterized by *through bond* interactions. In particular the SH and OH terminal bonds favor this type of interaction. Figure 7b shows that any departure from the equilibrium isomer (to go to trans or cis conformations) weakens the SO bond even though Figure 7a indicates that when going to the trans conformation $\rho_{bond}$ increases. Therefore in the gauche → trans path, the SH and OH bonds are strengthened, favoring the through bond type of interactions.

Let us now analyze the changes in chemical potential and hardness as functions of the specific Mulliken populations. Figure 8 shows $\mu$ and $\eta$ as functions of $\rho_{bond}$ and $\rho^{\circ}_{SO}$. Figure 8a,b indicates that any departure from the equilibrium conformation is accompanied by an increase in $\mu$ and a decrease in $\eta$, no matter what happens with the bond density. Seen as approaching the equilibrium conformation, $\mu$ tends to a minimum whereas $\eta$ tends to a maximum; these two condition can be fulfilled by different mechanisms that will affect the bond population in different ways. In particular, it is interesting to note that a decrease in hardness (the resistance to charge transfer) may be accompanied by the strengthening of the terminal chemical bonds, as is the case in the gauche → trans path. Opposite to this is the mechanism for the gauche → cis path, in which the terminal bonds are weakened.

The trends displayed by $\rho_{SO}$ and $\rho^{\circ}_{SO}$ in Figure 7b is indicate that the electronic population of the central bond should correlate with the profiles of chemical potential and hardness. In Figure 8c,d we show the results of linear correlations between $\mu$ and $\eta$ with $\rho^{\circ}_{SO}$. Figure 8(c) shows a quite good linear behavior of $\mu$ as a function of $\rho^{\circ}_{SO}$; note that this correlation can be improved when using a second-order polynomial. A distortion from the equilibrium conformation follows the arrow that indicate that it is associated with an increasing $\mu$ and a decreasing $\rho^{\circ}_{SO}$. In Figure 8(d) we show a remarkable linear relation between hardness and $\rho^{\circ}_{SO}$. Seen as a resistance to charge transfer, a decreasing hardness implies that the molecule will spontaneously distort owing to the weakness induced on the central bond.

## 4. Summary and Concluding Remarks

In this paper we have performed a theoretical study of the internal rotation of hydrogen thioperoxide. The isomerization process has been characterized through the evolution of the potential energy, chemical potential, and molecular hardness. Different procedures have been used to estimate $\mu$ and $\eta$ with the result that they lead to the same qualitative behavior; in particular, the RHF calculations using the Koopmans' theorem was found to be adequate to describe these electronic properties. We have obtained good estimations of barrier heights and properties associated with the stable isomer. An important result of this paper is that the PMH is verified even though $\mu$ varies along the reaction coordinate.

The mechanisms for departure from the equilibrium conformation have been characterized through an increasing $\mu$ and a decreasing $\eta$. This behavior, in connection with the change of some electronic populations, allows a qualitative identification of the specific intramolecular interactions that are at the origin of the physical nature of the two potential barriers.

Characterizing the nature of the potential barriers is a very difficult task because many effects and specific interactions should be rationalized correctly. We have shown that the information we obtain from the study of a chemical reaction in the $\{\mu, \eta, V\}$ space should be necessarily complemented by the information provided by the analysis of local electronic properties. There are different properties that can be used to predict stability and reactivity;[36] connection among them will provide new insight to help rationalize the chemical behavior of molecular systems.

**Acknowledgment.** The authors are grateful for financial support from FONDECYT through project No. 1961021/1996.

## References and Notes

(1) Parr, R. G.; Yang, W. *Annu. Rev. Phys. Chem.* **1995**, *46*, 701.
(2) Parr, R. G.; Pearson, R. G. *J. Am. Chem. Soc.* **1983**, *105*, 7512.
(3) Pearson, R. G. *J. Am. Chem. Soc.* **1985**, *107*, 6801.
(4) Pearson, R. G. *J. Chem. Educ.* **1987**, *64*, 561.
(5) Parr, R. G.; Yang, W. *Density Functional Theory of Atoms and Molecules*; Oxford University Press: New York 1989.
(6) Dreizler, R. M.; Gross, E. K. V. *Density Functional Theory*; Springer: Berlin, 1990.
(7) Chattaraj, P. K.; Nath, S.; Sannigrahi, A. B. *J. Phys. Chem.* **1994**, *98*, 9143.
(8) Cárdenas-Jirón, G. I.; Lahsen, J.; Toro-Labbé, A. *J. Phys. Chem.* **1995**, *99*, 5325.
(9) Cárdenas-Jirón, G. I.; Toro-Labbé, A. *J. Phys. Chem.* **1995**, *99*, 12730.
(10) Cárdenas-Jirón, G. I.; Gutiérrez-Oliva, S.; Melin J.; Toro-Labbé, A. *J. Phys. Chem. A* **1997**, *101*, 4621.
(11) Chattaraj, P. K. *Proc. Indian Natl. Sci. Acad.* **1996**, *62*, 513 and references therein.
(12) Pearson, R. G. *Chemical Hardness*; Wiley-VCH: Oxford, 1997.
(13) Datta, D. *J. Phys. Chem.* **1992**, *96*, 2409.
(14) Hammond, G. S. *J. Am. Chem. Soc.* **1955**, *77*, 334.
(15) Parr, R. G.; Chattaraj, P. K. *J. Am. Chem. Soc.* **1991**, *131*, 1854. Chattaraj, P. K.; Liu, G. H.; Parr, R. G. *Chem. Phys. Lett.* **1995**, *237*, 171.
(16) Pearson, R. G.; Palke, W. E. *J. Phys. Chem.* **1992**, *96*, 3283.
(17) Gázquez, J. L.; Mart′nez, A.; Méndez, F. *J. Phys. Chem.* **1993**, *97*, 4059.
(18) Nath, S.; Sannigrahi, A. B.; Chattaraj, P. K. *J. Mol. Struct.: THEOCHEM* **1994**, *309*, 65.
(19) Wayne, R. P., *Chemistry of Atmospheres*, 2nd ed.; Clarendon: Oxford, 1991.
(20) Balucani, N.; Beneventi, L.; Casavecchia, P.; Stranges, D.; Volpi, G. G. *J. Chem. Phys.* **1991**, *94*, 8611. Balucani, N.; N.; Casavecchia, P.; Stranges, D.; Volpi, G. G. *Chem. Phys. Lett.* **1993**, *211*, 469.

(21) Cárdenas-Jirón, G. I.; Toro-Labbé, A. *J. Mol. Struct.: THEOCHEM* **1997**, *390*, 79.
(22) Smardzewski, R. R.; Lin, M. C. *J. Chem. Phys.* **1997**, *66*, 3197.
(23) Iraqi, M.; Schwarz, H. *Chem. Phys. Lett.* **1994**, *221*, 359.
(24) Luke, B. T.; McLean, A. D. *J. Phys. Chem.* **1985**, *89*, 4592.
(25) Xantheas, S. S.; Dunning, T. H., Jr. *J. Phys. Chem.* **1993**, *97*, 18.
(26) O'Hair, R. A. J.; DePuy, C. H.; Bierbaum, V. M. *J. Phys. Chem.* **1993**, *97*, 7955.
(27) Goumri, A.; Rocha, J. D. R.; Laakso, D.; Smith, C. E.; Marshall, P. *J. Chem. Phys.* **1994**, *101*, 9405.
(28) Marcus, R. A. *Annu. Rev. Phys. Chem.* **1964**, *15*, 155.
(29) Dodd, J. A.; Brauman, J. I. *J. Phys. Chem.* **1986**, *90*, 3559.
(30) Frisch, M. J.; Trucks, G. W.; Schlegel, H. B.; Gill, P. M. W.; Johnson, B. G.; Robb, M. A.; Cheeseman, J. R.; Keith, T. A.; Peterson, G. A.; Montgomery, J. A.; Raghavachari, K.; Al-Laham, M. A.; Zakrzewski, V. G.; Ortiz, J. V.; Foresman, J. B.; Ciolowski, J.; Stefanov, B. B.; Nanayakkara, A.; Challacombe, M.; Peng, C. Y.; Ayala, P. Y.; Chen, W.; Wong, M. W.; Andres, J. L.; Reploge, E. S.; Gomperts, R.; Martin, R. L.; Fox, D. J.; Binkley, J. S.; Defrees, D. J.; Baker, J.; Stewart, J. P.; Head-Gordon, M.; González, C.; Pople, J. A. *Gaussian 94*: Gaussian Inc.: Pittsburgh, PA, 1995.
(31) Pal, S.; Vaval, N.; Roy, R. *J. Phys. Chem.* **1993**, *97*, 4404.
(32) Chattaraj, P. K.; Nath, S.; Sannigrahi, A. B. *Chem. Phys. Lett.* **1993**, *212*, 223.
(33) Nath, S.; Sannigrahi, A. B.; Chattaraj, P. K. *J. Mol. Struct.: THEOCHEM* **1994**, *306*, 87.
(34) Hunt, R. H.; Leacock, R. A.; Peters, C. W.; Hecht, K. T. *J. Chem. Phys.* **1965**, *42*, 1931.
(35) Pelz, G.; Yamada, K. M. T.; Winnewisser, G. *J. Mol. Spectrosc.* **1993**, *159*, 507.
(36) Ghanty, T. K.; Ghosh, S. K. *J. Phys. Chem.* **1996**, *100*, 12295, 17429; *Int. J. Quantum Chem.* **1997**, *63*, 917.